BIOCHEMISTRY
including biophysical chemistry & molecular biology

Article

pubs.acs.org/biochemistry

Probing the Molecular Architecture of *Arabidopsis thaliana* Secondary Cell Walls Using Two- and Three-Dimensional ^{13}C Solid State Nuclear Magnetic Resonance Spectroscopy

Ray Dupree,[†] Thomas J. Simmons,[‡] Jennifer C. Mortimer,[‡] Dharmesh Patel,[†,‡] Dinu Iuga,[†] Steven P. Brown,[†] and Paul Dupree*[,‡]

[†]Department of Physics, University of Warwick, Coventry CV4 7AL, U.K.

[‡]Department of Biochemistry, University of Cambridge, Tennis Court Road, Cambridge CB2 1QW, U.K.

Supporting Information

ABSTRACT: The plant secondary cell wall is a thickened polysaccharide and phenolic structure, providing mechanical strength to cells, particularly in woody tissues. It is the main feedstock for the developing bioenergy and green chemistry industries. Despite the role that molecular architecture (the arrangement of biopolymers relative to each other, and their conformations) plays in dictating biomass properties, such as recalcitrance to breakdown, it is poorly understood. Here, unprocessed dry ^{13}C-labeled stems from the model plant *Arabidopsis thaliana* were analyzed by a variety of ^{13}C solid state magic angle spinning nuclear magnetic resonance methods, such as one-dimensional cross-polarization and direct polarization, two-dimensional refocused INADEQUATE, RFDR, PDSD, and three-dimensional DARR, demonstrating their viability for the study of native polymer arrangements in intact secondary cell walls. All carbon sites of the two main glucose environments in cellulose (previously assigned to microfibril surface and interior residues) are clearly resolved, as are carbon sites of the other major components of the secondary cell wall: xylan and lignin. The xylan carbon 4 chemical shift is markedly different from that reported previously for solution or primary cell wall xylan, indicating significant changes in the helical conformation in these dried stems. Furthermore, the shift span indicates that xylan adopts a wide range of conformations in this material, with very little in the 3_1 conformation typical of xylan in solution. Additionally, spatial connections of noncarbohydrate species were observed with both cellulose peaks conventionally assigned as "surface" and as "interior" cellulose environments, raising questions about the origin of these two cellulose signals.

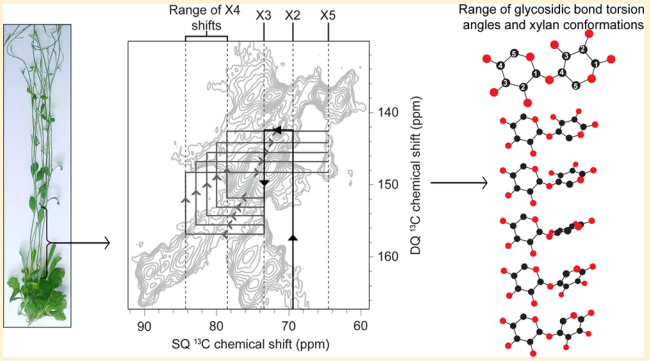

In woody plant tissues, a secondary cell wall is laid down on the interior of the thin, extensible, and biochemically and functionally distinct primary cell wall during cellular differentiation. The secondary wall is crucial to many aspects of plant physiology, including mechanical strength. It also comprises the vast majority of the material of mature plant tissues and lignocellulosic biomass and is therefore an invaluable resource for renewable materials and for bioenergy feedstocks.[1,2]

The polysaccharide components of the cell wall, which constitute more than 60% of its dry weight, are commonly categorized into three constituent types: cellulose, hemicellulose, and pectin.[3,4] Cellulose is thought to be the main load-bearing structure of the cell wall and is the most abundant polymer in both primary and secondary walls.[5] Cellulose chains are composed of β-(1→4)-D-glucosyl residues (Figure 1) that are partly assembled into layers in a microfibril by inter- and intrachain hydrogen bonding and hydrophobic interactions. Within crystalline regions of cellulose microfibrils (known as crystallites), glucan chains are found in a 2-fold (2_1) helical conformation, in which each residue is rotated 180° around the glycosidic bond relative to the residue on either side of it. Two allomorphs of crystalline cellulose are known to occur in plant cellulose: the single-chain triclinic Iα crystal and the two-chain monoclinic Iβ crystal.[6−8] Solid state magic angle spinning (MAS) nuclear magnetic resonance (ssNMR) suggests that the latter predominates in plant cellulose,[9] but a recent X-ray diffraction study suggests that cellulose Iα and Iβ stacking patterns may coexist within each microfibril.[10] Despite many years of study, the number of chains in a plant cellulose microfibril and the nature of the fibril faces have remained poorly defined. NMR spectra can show multiple signals for some cellulose carbons, indicating multiple glucose environments (e.g., Atalla and VanderHart[6] and Wickholm et al.[11]). The differing cellulose carbon 4 (C4) and C6 signals

Received: December 22, 2014
Revised: March 2, 2015
Published: March 4, 2015

DOI: 10.1021/bi501552k
Biochemistry 2015, 54, 2335−2345

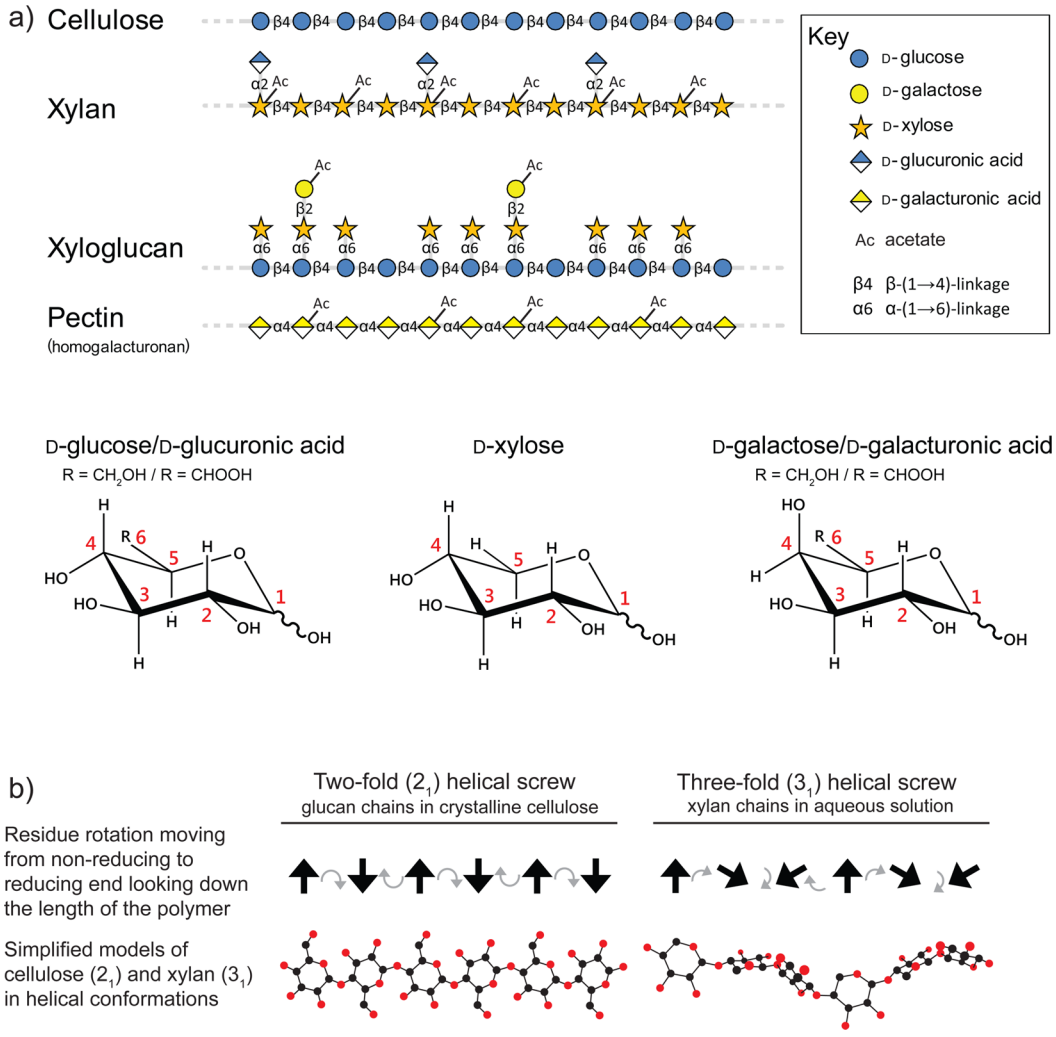

Figure 1. Models of the molecular structures and physical conformations of pertinent polysaccharides and their constituent monosaccharides. (a) Molecular structures of *Arabidopsis* polysaccharides discussed in this work. Cellulose is found as a semicrystalline aggregate of multiple individual chains; all other polysaccharides can, in principle, be found as soluble individual polymers. Xylan and xyloglucan are both classified as hemicellulosic polysaccharides. Xylan is the most predominant hemicellulose in the dicot secondary cell wall and xyloglucan that in the dicot primary cell wall. Along the majority of the xylan polymer acetylation occurs on every second xylose residue, and even numbers of xylose residues separate glucuronosyl decorations. The pectin model is of the homogalacturonan portion of pectin; the pattern of acetylation of pectin is assumed to be random. All monosaccharides are found in the pyranosyl configuration. (b) Models of 2-fold (2_1) and 3-fold (3_1) helical polysaccharide conformations, with cellulose and xylan as examples.

(frequently seen as doublets) are often assigned to interior and surface polymer chains.[12,13] Reasons that interior and surface chains might exhibit these different NMR chemical shifts include the fact that the C6 hydroxymethyl group might adopt different orientations relative to the ring when on the surface compared to when part of the crystalline interior[14] and the fact that glycosidic bond angles on surface chains might differ from those typical for the conventional 2_1 conformation of interior cellulose chains.[15] An alternative explanation that has been suggested for the "surface" signal is the existence of noncrystalline "amorphous" regions in the fibrils, or regions with structural defects.[16,17] Such amorphous regions could yield divergent C4 and C6 signals by both variations in glycosidic bond conformation and/or C6 hydroxymethyl rotation.

The hemicelluloses are a diverse range of polysaccharides hypothesized to partially coat the cellulose microfibrils and/or to tether adjacent microfibrils, thus contributing to the load-bearing structure of the cell wall.[3] The major hemicellulose in primary cell walls of dicot plants (such as *Arabidopsis*) is xyloglucan, while that of the dicot secondary cell walls is xylan, a polymer of β-(1→4)-D-xylosyl residues partly substituted with [4-*O*-Me]-α-D-glucuronic acid and acetyl groups (Figure 1). The pectins are a group of heavily charged anionic polysaccharides composed of galacturonosyl and other residues, and they are less abundant in secondary cell walls than primary cell walls. Another major difference from primary cell walls is that mature secondary cell walls undergo lignification, in which phenolic monolignols are oxidatively cross-linked in the wall to form a complex network. Lignin is the major noncarbohydrate component of lignocelluloses as well as a major causal factor in biomass recalcitrance (resistance to chemical breakdown).[18,19]

Despite the prevalence and importance of plant cell wall material and in contrast to the detailed understanding of its composition, there is currently a distinct lack of a clear understanding of plant cell wall molecular architecture (the polymer conformations and how these components are arranged relative to each other) and how this contributes to cell wall mechanical properties and recalcitrance.[20−24] One

DOI: 10.1021/bi501552k
Biochemistry 2015, 54, 2335−2345

particularly interesting aspect is the nature of interactions between the two most predominant polymers of the dicot secondary wall: xylan and cellulose. The molecular similarities between glucose and xylose (Figure 1) hint at the feasibility of extended interactions between cellulose and xylan chains, like those that occur between adjacent cellulose chains within a crystalline microfibril. However, side-chain decorations of xylan could obstruct such extended interactions, and so too might conformational discrepancies between the polymer types: in contrast to the 2_1 conformation (two residues per 360° twist) of crystalline cellulose, xylan is known to exist in a 3_1 conformation (three residues per 360° twist) in solution, and homoxylan crystallizes in this conformation[25] (Figure 1). The discovery by Bromley et al.[26] and Busse-Wicher et al.[27] that, for the majority of the polymer, only alternate xylosyl residues carry glucuronosyl or acetyl substitutions could reconcile these issues. They hypothesized that the even-numbered spacing of decorations along the xylan chain may allow xylan to align with a 2_1 conformation in a crystal-like manner on the face of cellulose microfibrils, with substitutions facing the lignin-rich matrix. However, there is little evidence concerning the conformation of xylan in cell walls, and any tools that could detect native polysaccharide conformations within intact cell walls would prove to be invaluable to future investigations into cell wall architecture.

One reason for this dearth of evidence is the practical limitations of testing molecular architecture hypotheses; the disruptive chemical and biochemical methods employed for elucidation of the composition of cell walls are not amenable to such investigations. Solid state NMR (ssNMR), however, does have the potential to yield information about the native arrangement of cell wall components because this technique does not necessitate potentially disruptive preparation. Furthermore, NMR is useful for probing the conformation of carbohydrates, as 2_1 and 3_1 conformations in (1→4)-linked glycans have been shown to exhibit characteristic changes in C4 resonances.[28] Hong and colleagues have pioneered the use of multidimensional ssNMR to probe the molecular architecture of the primary cell walls of uniformly ^{13}C-labeled *Arabidopsis* hypocotyls.[29−33] They and others show and suggest that only a minor part of the main hemicellulose, xyloglucan, interacts with cellulose, challenging conventional models of the primary cell wall.[29,32,34] ssNMR studies of secondary cell walls have been less intensive: some have used one-dimensional (1D) ssNMR to analyze the distinct secondary cell walls of *Arabidopsis*,[35] spruce wood,[21] and maize.[36] However, the limited resolution afforded by 1D ssNMR makes it difficult to distinguish the many peaks that share similar chemical shifts. The better resolution of two-dimensional (2D) ssNMR has been exploited to study the industrially important secondary cell wall of aspen[37,38] and maize.[39] However, thorough ssNMR studies of the native secondary cell wall of the model plant *Arabidopsis* are the most pressing, as these would contribute most to our understanding of the roles of the secondary cell wall biosynthetic machinery, as well as benefit from the large suite of biochemically characterized *Arabidopsis* cell wall synthesis mutants.

Here the first multidimensional ssNMR analyses of untreated secondary cell wall-rich *Arabidopsis* stems are reported. ^{13}C-labeled *Arabidopsis* material was studied using a variety of ^{13}C ssNMR methods, showing that the technique can probe the molecular environments of cellulose and xylan in the native secondary cell wall. Signals corresponding to a range of cell wall polymers, including xylan and the characteristic two domains of cellulose, were observed. Interestingly, the chemical shifts of xylan differed significantly from those from previous solution and primary cell wall studies. This indicates that xylan is found in distinct conformations in dried plant cell walls. It was also possible to identify intermolecular spatial connections between cellulose and other cell wall components.

EXPERIMENTAL PROCEDURES

Sample Preparation. Mature uniformly ^{13}C-labeled (approximately 99%) lyophilized wild-type *Arabidopsis* Columbia-0 stems were purchased from IsoLife (Wageningen, The Netherlands), and 50 mg was chopped and packed into a 4 mm MAS NMR zirconia rotor.

Monosaccharide Analysis. Portions (1 mg) of three independent ^{13}C-labeled *Arabidopsis thaliana* stems were separately homogenized in 96% (v/v) ethanol using a ball mill. Insoluble material was precipitated by centrifugation before being resuspended and thoroughly vortexed in 1.5 mL of 75% (v/v) ethanol. Precipitation followed by resuspension was then repeated five times before the remaining insoluble material was dried *in vacuo*. Each of the three alcohol-insoluble residues was then subjected to trifluoroacetic acid (TFA) hydrolysis and high-performance anion-exchange chromatography (HPAEC) analysis as described previously.[40]

Solid State NMR. MAS solid state NMR experiments were performed on a widebore Bruker (Karlsruhe, Germany) AVANCE III 850 MHz solid state NMR spectrometer operating at 20 T, corresponding to ^{1}H and ^{13}C Larmor frequencies of 850.2 and 213.8 MHz, respectively, using a 4 mm double-resonance MAS probe. Experiments were conducted at room temperature at a MAS frequency of 14.0 kHz ± 5 Hz unless otherwise stated. The ^{13}C chemical shift was determined using the carbonyl peak at 177.8 ppm of L-alanine as an external reference with respect to TMS; 90° pulse lengths of typically 3.5 μs (^{1}H) and 3 μs (^{13}C) were used. Two-pulse phase-modulated (TPPM) decoupling[41] was applied during acquisition at a ^{1}H nutation frequency of 83 kHz with a recycle delay of 2 s unless otherwise stated. All spectra obtained were processed and analyzed using Bruker Topspin version 3.2.

1D ^{13}C CP/DP MAS NMR. 1D ^{13}C cross-polarization (CP) MAS spectra were recorded with an 18 ms acquisition time, with a spectral window of 55 kHz (260 ppm) and 32 co-added transients, whereas 256 transients were acquired for the direct-polarization (DP) spectra. Cross-polarization preferentially improves the signal for more rigid cell wall components, whereas DP with a 20 s recycle delay is needed for a quantitative spectrum. For ^{1}H−^{13}C CP experiments, transverse magnetization was created using ramped (70−100%) cross-polarization[42] from ^{1}H with a contact time of 1 ms. Data were Fourier transformed into 2K complex data points, and exponential multiplication (EM) line broadening of 60 Hz was applied during processing.

2D ^{13}C−^{13}C Refocused INADEQUATE NMR. Two-dimensional double-quantum (DQ) correlation spectra were recorded using the refocused INADEQUATE pulse sequence,[38,43] which relies upon the use of isotropic, scalar *J* coupling to obtain through-bond information regarding directly coupled nuclei. Ramped cross-polarization with a contact time of 1 ms was used to transfer magnetization from ^{1}H to ^{13}C with SPINAL-64 decoupling[44] during evolution and signal acquisition periods. Carbon 90° and 180° pulse lengths of 3 and 6 μs, respectively, were used with a τ delay of 2.2 ms. A spectral width of 56 kHz

DOI: 10.1021/bi501552k
Biochemistry 2015, 54, 2335−2345

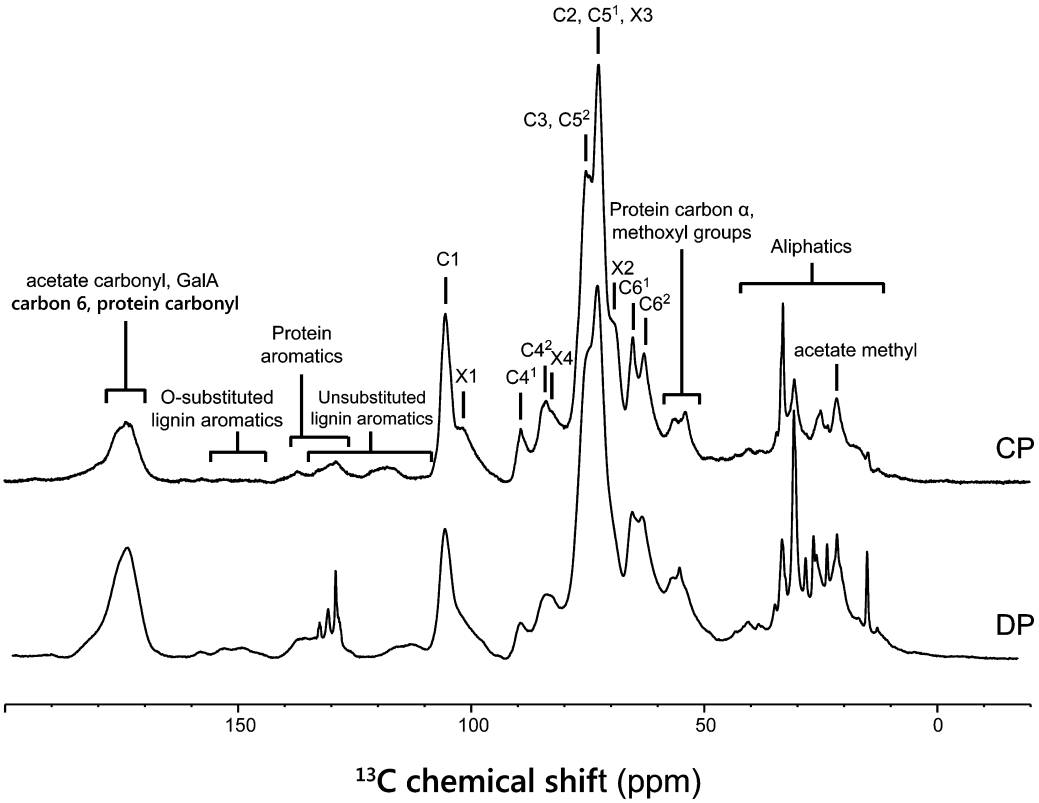

Figure 2. ^{13}C solid state MAS NMR spectra of intact isotopically ^{13}C-enriched secondary cell wall-rich *Arabidopsis* stems obtained by cross-polarization (CP, top) and direct polarization (DP, bottom). Spectra were scaled to similar intensities on the basis of the major signal at 72 ppm. Resonances were initially assigned on the basis of the literature. C and X refer to carbons in cellulose and xylan, respectively. Spectra were recorded on an 850 MHz spectrometer with a MAS frequency of 14 kHz and a recycle delay of 2 s for CP and 20 s for DP.

was used in both dimensions, and spectra were acquired with 2K complex data points in F_2 and 96 transients co-added for each of the 460 increments in t_1 using the TPPI method for sign discrimination. The recycle delay was 1.5 s, resulting in a total experimental time of 21 h. The data obtained were Fourier transformed into 2K (F_2) × 1K (F_1) points with EM line broadening of 20 Hz in F_2 and squared sine bell in F_1.

2D $^{13}C-^{13}C$ RFDR NMR. The radiofrequency-driven recoupling (RFDR) experiment[45] uses rotor-synchronized π pulses on ^{13}C during the mixing period to reintroduce homonuclear $^{13}C-^{13}C$ dipolar couplings that are averaged out under MAS. A short mixing time was chosen so as to reintroduce only selectively short-range dipolar couplings between directly bonded neighboring carbon atoms. The rotor-synchronized 180° pulse on the ^{13}C channel during mixing was set to 6 μs, with one rotor period being 76.9 μs (13 kHz MAS). The mixing time was set to 2.308 ms (30 rotor periods). A spectral window of 64 kHz (~300 ppm) was used in both dimensions, and spectra were acquired with 2K data points in F_2 with 72 co-added transients for each of the 782 t_1 increments using TPPI. The acquisition time was 16 ms in F_2 and 6.2 ms in F_1 with a recycle delay of 1.5 s, giving a total experimental time of ~24 h. As evidenced by the spectrum obtained, only short-range couplings over a single bond distance (~1.5−2 Å) were observed.

Three-Dimensional (3D) $^{13}C-^{13}C-^{13}C$ CP DARR NMR Experiments. Dipolar-assisted rotational recouping (DARR) spectroscopy[46] assists the spin diffusion process by using a combination of physical rotation of the sample and the application of continuous low-power radiofrequency pulses on the proton channel at a ^1H nutation frequency corresponding to the $n = 1$ rotary resonance during the mixing time (t_{mix}). This reintroduces dipolar couplings that are typically averaged out by MAS, thereby allowing the observation of long-range $^{13}C-^{13}C$ contacts at long mixing times. A 3D $^{13}C-^{13}C-^{13}C$ DARR experiment was used to further aid resolution and to probe spatial relationships between components in the cell wall. In this experiment, there are two mixing times, t_{m1} and t_{m2}, where t_{m1} is short (~10 ms) and t_{m2} can be either short or long.[47] A long t_{m2} allows the observation of both intramolecular and intermolecular correlations, while for a short t_{m2}, only intramolecular connections should be visible. Two 3D DARR experiments were undertaken, one with both t_{m1} and t_{m2} equal to 10 ms and the other with a t_{m1} of 10 ms and a t_{m2} of 300 ms. The spectral width was set to 64 kHz (300 ppm) in direct dimension F_3 and to the spinning frequency, 14 kHz (65.5 ppm), in indirect dimensions F_2 and F_1. SPINAL-64 proton decoupling was applied during signal acquisition. Data were acquired for 16 ms in the direct dimension (F_3) and with 128 increments (4.6 ms) and 107 increments (3.8 ms) in indirect dimensions F_2 and F_1, respectively, using States acquisition in F_2 and States-TPPI in F_1 with mixing times (t_{m1} and t_{m2}) of 10 ms, and with 90 increments (3.2 ms) in F_1 for the experiment with a t_{m2} of 300 ms. Sixteen transients were co-added for each t_1 and t_2 increment, giving total experimental times of ~4.5 and 5.5 days, respectively.

DOI: 10.1021/bi501552k
Biochemistry 2015, 54, 2335−2345

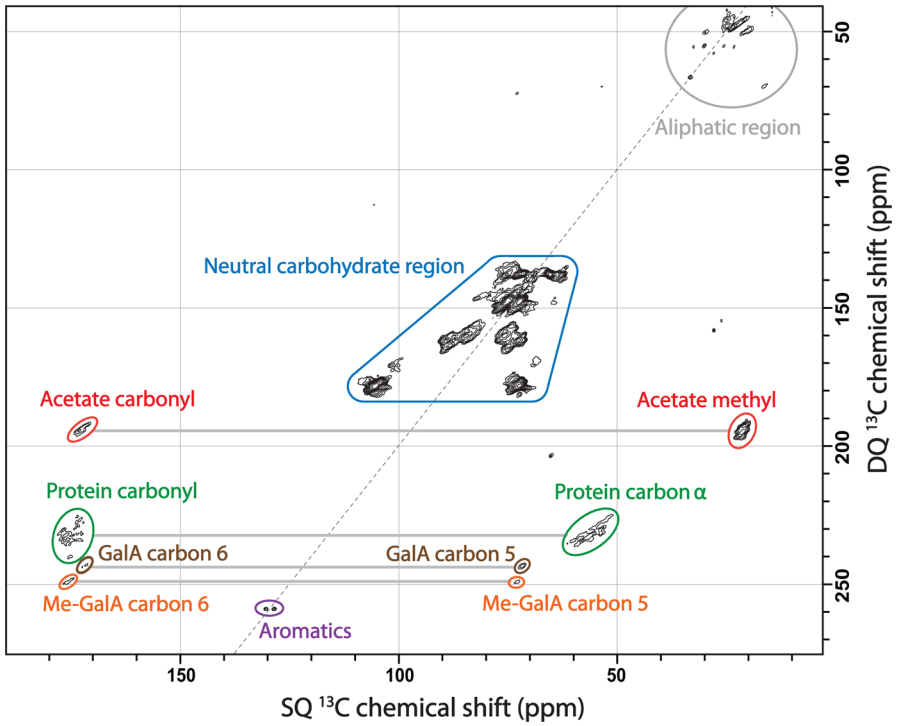

Figure 3. 2D $^{13}C-^{13}C$ CP refocused INADEQUATE spectrum (850 MHz, 14 kHz MAS) showing the full range of moieties detected in *Arabidopsis* secondary cell walls. The carbonyl region 170−180 ppm was resolved into acetate carbonyl groups, protein carbonyl groups, and uronic acid carbonyl groups, all identified by *J* coupling to bonded carbons. The uronic acid carbonyl groups were comprised of two distinct groups, identified from the literature as methyl-esterified and non-methyl-esterified galacturonic acid of pectin.

RESULTS

Assignment of Resonances from *Arabidopsis* Secondary Cell Walls. *Holistic Wall Overview.* Mature *Arabidopsis* stems are a widely used model for studies of secondary cell walls, which contain substantial proportions of cellulose, xylan, and lignin, as well as some protein and pectin.[19,48] To support ssNMR analyses of mature uniformly ^{13}C-labeled lyophilized *Arabidopsis* stems, the monosaccharide composition of the noncrystalline polysaccharides (i.e., hemicellulose, pectin, and amorphous cellulose) was assessed by TFA hydrolysis followed by HPAEC (Figure S1 of the Supporting Information). Xylose was the main monosaccharide, indicating that the stems had a high xylan content, as is typical of *Arabidopsis* secondary cell wall-rich material.[48] The intact, unprocessed uniformly ^{13}C-labeled stems were then analyzed via a range of ssNMR experiments. All assigned resonances are given in Table S1 of the Supporting Information together with literature values where available.

1D ^{13}C ssNMR spectra gave an initial holistic assessment of the components of the secondary cell wall. A comparison of quantitative DP and the more sensitive CP spectra is shown in Figure 2. As expected, we observed peaks indicative of carbonyl (170−180 ppm), aromatic (105−150 ppm), neutral carbohydrate (60−110 ppm), methoxyl groups/protein Cα (50−60 ppm), and aliphatic (10−40 ppm) carbons. These shifts are consistent with those previously reported from 1D ssNMR studies of *Arabidopsis* primary cell walls and woody, secondary cell walls from various species.[15,31,32,35] Notably, a higher proportion of aromatic and aliphatic/protein components is evident in these secondary cell walls in comparison to the *Arabidopsis* primary wall samples studied by Dick-Perez and colleagues.[29,30] This is probably because proteins had been removed from the primary cell wall samples by extraction in their work. Furthermore, the secondary cell walls of *Arabidopsis* stems contain substantial amounts of the aromatic component lignin, which is absent from primary cell walls.[18,19] The lower intensity of carbonyl, aromatic, and protein peaks in the CP spectrum, which is less sensitive to mobile species, indicates that some of these components have high mobility.

The 1D ^{13}C spectra are congested and do not allow confident assignment of many components. However, the high sensitivity arising from ^{13}C labeling of the *Arabidopsis* stems enabled employment of an assortment of multidimensional NMR experiments to probe the composition of the secondary cell walls. We first investigated whether CP refocused INADEQUATE of the intact, unprocessed dried material could allow sufficient resolution for further assignment. Indeed, Figure 3 shows that many carbon signals are remarkably well resolved. The carbonyl peak at 170−180 ppm comprised signals representative of three constituents: carbonyl of acetate, which mainly esterifies xylan and pectin;[49] carbonyl of protein, probably both in the cell wall and inside the cell; and Carbon 6 of uronic acids, mostly galacturonic acid of pectin. The acetate carbonyl component (173.1 ppm) was identified by its *J* coupling to methyl groups at ∼21 ppm. Similarly, the protein carbonyl component (a diffuse peak at 171−179 ppm) was *J* coupled to protein Cα at 49−66 ppm. Pectic galacturonic acid Carbon 6 components (both methyl-esterified and un-methyl-esterified; 175.5 and 171.5 ppm, respectively), belonging to homogalacturonan and probably also rhamnogalacturonan I, are *J* coupled to galacturonic acid Carbon 5 atoms at ∼73.2 and ∼71.9 ppm. Lignin aromatic carbons O-substituted with methoxyl groups have shifts of around 145−155 ppm, and unsubstituted carbons have shifts varying between 105 and 135 ppm.[50,51] However, the signal is weak in the ^{13}C CP

DOI: 10.1021/bi501552k
Biochemistry 2015, 54, 2335−2345

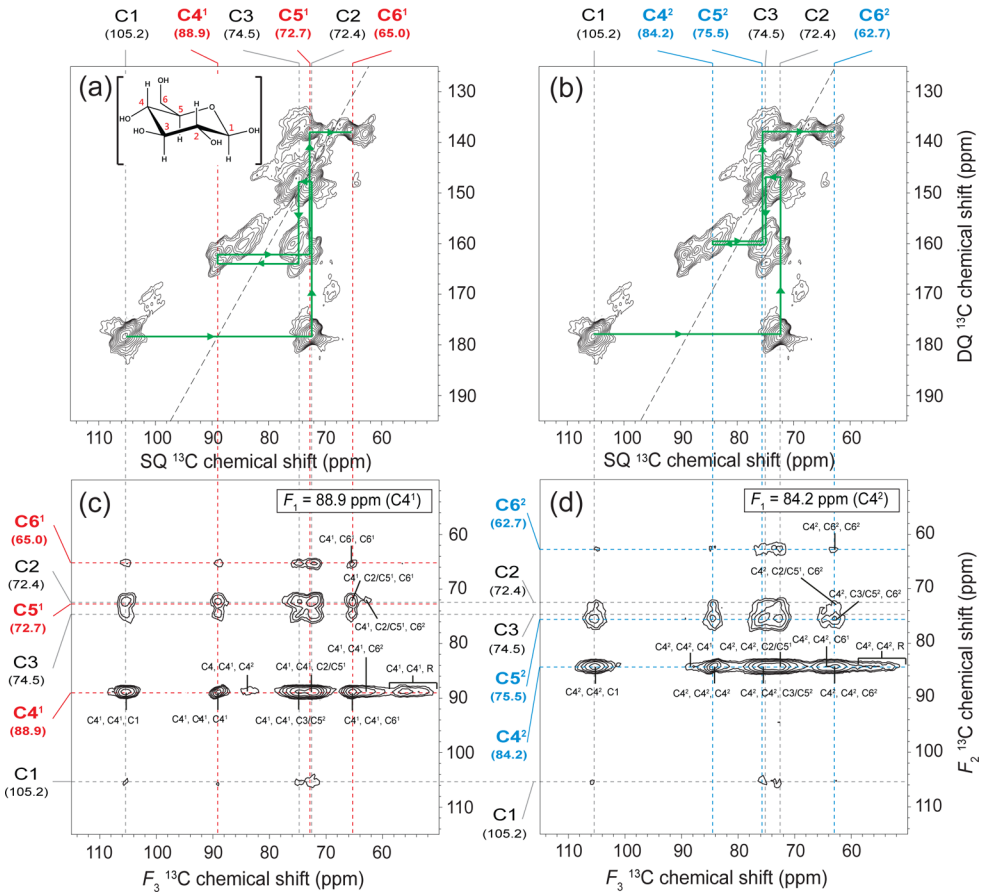

Figure 4. 2D $^{13}C-^{13}C$ CP refocused INADEQUATE (a and b) and 2D planes from 10 to 300 ms 3D $^{13}C-^{13}C-^{13}C$ DARR (850 MHz, 14 kHz) (c and d) spectra showing intra- and interconnectivities of the cellulose domains within *Arabidopsis* secondary cell walls. (a) Cellulose domain 1. The inset shows *β*-D-glucose. (b) Cellulose domain 2. (c) $C4^1$ interconnectivities, largely in cellulose domain 1. (d) $C4^2$ interconnectivities, largely in cellulose domain 2. Lines show chemical shifts of specific carbons with carbon identity, and shift values in parentheses, shown. Carbons in bold are those that vary between the two domains. Peaks on the DARR planes are labeled in the order F_1, F_2, F_3.

INADEQUATE spectrum, so that only the aromatic groups at ~130 ppm are visible.

The biomass in mature *Arabidopsis* stems is largely composed of secondary cell walls, but primary cell wall polymers are present in small quantities.[35,48] In the ^{13}C refocused INADEQUATE spectra, we were unable to detect the terminal xylose Carbon 4−Carbon 5 connection (70.5 ppm-to-62.3 ppm) identified by Dick-Perez et al.[29] as being indicative of xyloglucan and thus conclude that primary cell wall polysaccharides, of which xyloglucan is a major component, cannot easily be detected. Thus, the moieties that are observed are mainly secondary wall polymers. The fact that galacturonic acid was readily detected is probably owed to pectin's additional prevalence in the middle lamella of mature stems.[52]

Spatial Connectivities within and between Two Cellulose Domains. The most intense and heavily congested peaks in the ^{13}C refocused INADEQUATE spectra are in the neutral carbohydrate region (Figure 3), reflecting the high carbohydrate content of the cell walls. The major peaks are consistent with those previously assigned to cellulose[29] (Figure 4). These include the anomeric cellulose C1 (105.1 ppm), the C4 region (84−89 ppm), the region of C2, C3, and C5 (70−80 ppm), and the C6 region (62−65 ppm). In the refocused INADEQUATE spectra, C4 (84.2 and 88.9 ppm), C5 (72.7 and 75.5 ppm), and C6 (62.7 and 65.0 ppm) show two clearly resolved peaks present in distinct spin systems, reflecting two differing environments of glucose in the cellulose microfibrils (Figure 4a,b). These glucose environments are conventionally assigned to cellulose chains on the interior or surface of cellulose microfibrils.[29] Alternatively, as discussed earlier, they are sometimes assigned to crystalline or amorphous regions of microfibrils.[17] Given the ambiguities about the nature of the two domains, we refer to them simply as cellulose domain 1 ($C4^1$, 88.9 ppm; $C5^1$, 72.7 ppm; $C6^1$, 65.0 ppm) and cellulose domain 2 ($C4^2$, 84.2 ppm; $C5^2$, 75.5 ppm; $C6^2$, 62.7 ppm) (Table S1 of the Supporting Information).

The spatial proximity of glucosyl residues in the two cellulose domains was probed by assessing the transfer of magnetization from C4 of glucose in domain 1 or domain 2 using 3D $^{13}C-^{13}C-^{13}C$ DARR experiments (Figure 4c,d). $C4^1$ (plane at 88.9 ppm) showed magnetization transfer, within a t_{m1} of 10 ms, to $C6^1$ (65.0 ppm) but not significantly to $C6^2$ (62.7 ppm), indicating that $C4^1$ is more closely associated with $C6^1$ than $C6^2$, consistent with $C4^1$ and $C6^1$ being in the same glucosyl residue of cellulose domain 1. In the third dimension (t_{m2} = 300 ms), there was transfer of magnetization from $C4^1$ to the 63 ppm region encompassing $C6^2$. Likewise, there was transfer from $C4^1$ to $C4^2$ (84.2 ppm) in a t_{m2} of 300 ms but not in 10 ms. The transfer from glucose domain 1 to domain 2 after longer mixing times indicates the spatial proximity of some glucosyl residues in the two cellulose domains. Similarly, with respect to glucose in domain 2, magnetization transfer from

DOI: 10.1021/bi501552k
Biochemistry 2015, 54, 2335−2345

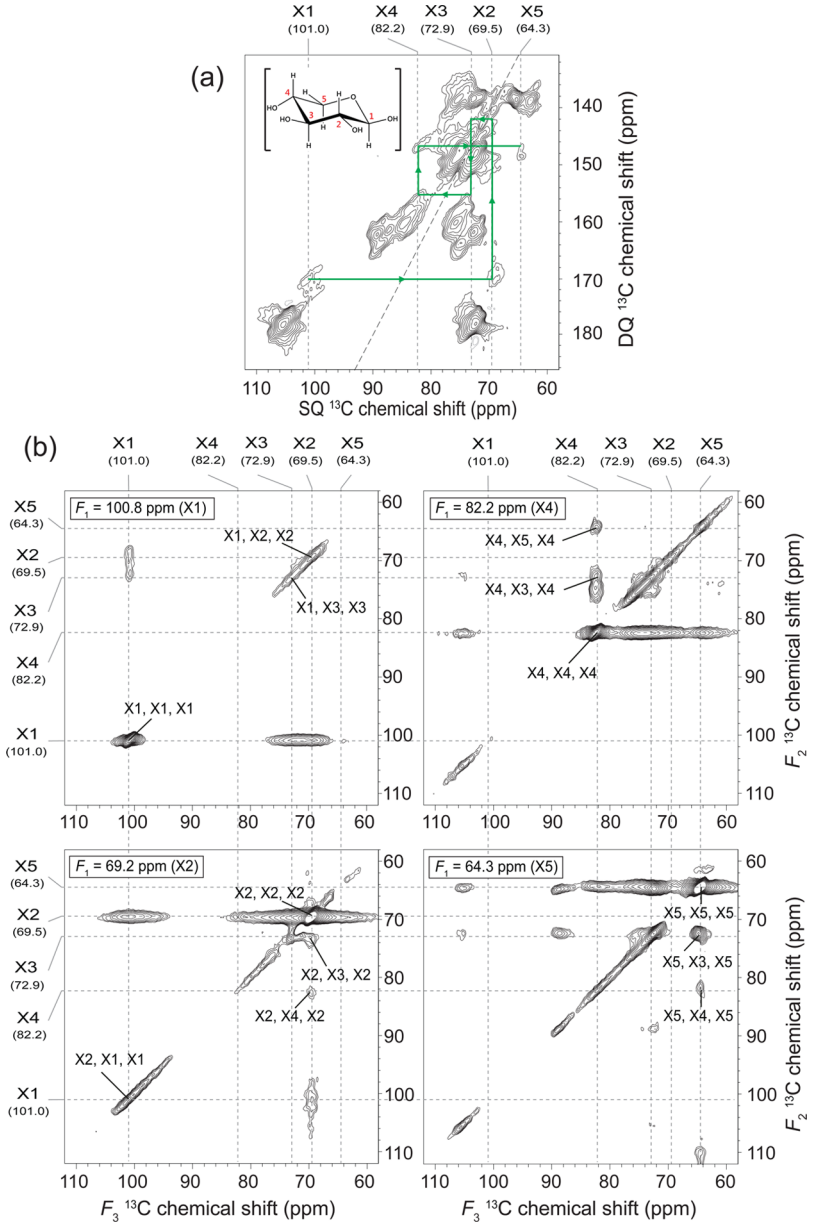

Figure 5. Assignment of xylosyl residues of xylan using ^{13}C CP refocused INADEQUATE (a) and 2D planes from a 3D 10 ms−10 ms ^{13}C−^{13}C−^{13}C DARR spectrum showing transfer between xylan nuclei (b). The inset in panel a is *β*-D-xylose. Peaks on the DARR planes are labeled in the order F_1, F_2, F_3.

$C4^2$ (plane at 84.2 ppm) showed transfer, within a t_{m1} of 10 ms, to $C6^2$ (62.7 ppm) (Figure 4d). At longer mixing times (300 ms), there was transfer of magnetization from $C4^2$ to $C4^1$ (88.9 ppm) and the $C6^1$ region. This too indicates the spatial proximity of the two cellulose domains (Figure 4d). It was also possible to assign from the refocused INADEQUATE experiment another less abundant domain with similar chemical shifts (see Table S1 of the Supporting Information) to those found recently in primary cell walls and called "interior 2".[31]

Xylan. A set of five resonances were assigned to the xylose of xylan (Figures 1 and 5). Connections xylose carbon 1 to xylose carbon 2 (X1 to X2) and X4 to X5 were unambiguously identified from cross-peaks in refocused INADEQUATE (Figure 5a) and RFDR (Figure S2 of the Supporting Information) spectra. Cross-peaks in a 10 ms−10 ms 3D DARR spectrum support these assignments, show connections between these two pairs (e.g., X2 to X4), and identify connections to X3 (Figure 5b). The absence of a *J* coupling between X5 and a putative uronic acid carbon 6 (which would be ∼175 ppm) ruled out the possibility that X1−X5 are the first five carbons of a uronic acid hexose, such as galacturonic acid (Figure 3). Finally, the intensity of these peaks further supports the possibility of their source being xylan, the main non-cellulosic component of the secondary cell wall (Figure S1 of the Supporting Information). On further analysis of the refocused INADEQUATE spectrum (see Figure 6), the shapes of the X4−X5 correlation peaks clearly indicate that there is a distribution in X4 shifts[53−55] (SQ values of ∼79−84 ppm with a range of DQ values from ∼143 to 148 ppm), all of which are bonded to X5 with a nearly constant shift of ∼64.3 ppm. In previous work, varying degrees of xylan substitution with acetate and 4-*O*-methylglucuronic acid were found to alter X1−X4 shifts in aqueous solution, but the change in X4 shift was only 1 ppm.[27,56] The exceptionally large range of 5 ppm for the

DOI: 10.1021/bi501552k
Biochemistry 2015, 54, 2335−2345

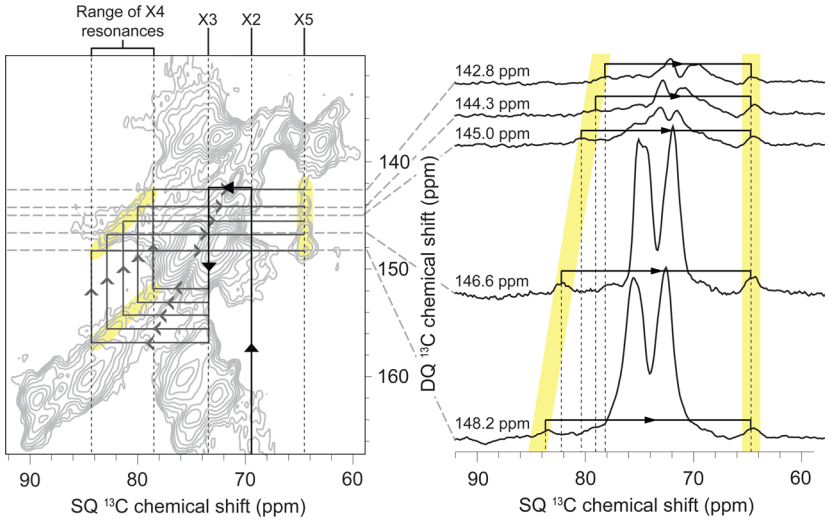

Figure 6. Xylosyl residues of xylan exhibit a range of X4 chemical shifts, suggestive of a range of different environments or folds. The left panel shows the ^{13}C CP refocused INADEQUATE spectrum indicating the xylan assignment with proposed ranges of xylan shifts highlighted in yellow. The large range of X4 resonances is probably due to a range of glycosidic bond conformations. The smaller variation in resonances of the other carbons could be from backbone decorations. Individual arrows X3 → X4 and X4 → X5 are illustrative of the range only; they do not indicate distinct observable connections. In the right panel, slices from the CP refocused INADEQUATE spectrum show the range of DQ values for which the 64 ppm peak (X5) is correlated with the proposed X4 resonances.

X4 shift is therefore likely to arise instead from xylan conformational variations in the cell wall.

Spatial Arrangements of Different Secondary Cell Wall Components. Proximity of Cellulose to Lignin, Protein and Pectin. Additional spatial arrangements shed initial light on the molecular architecture of the secondary cell wall. During the t_{m1} = 300 ms mixing time of a 3D DARR experiment, transfer of magnetization from cellulose C4^1 and C4^2 indicated their spatial proximity to peaks that span the methoxyl group and protein Cα region (Figures 4c,d and 7; labeled R). C4^1 ("interior cellulose") has a link to these groups somewhat stronger than that of C4^2 ("surface cellulose"). The two resolved peaks at 53 and 56 ppm seen in the 1D NMR spectra (Figure 2) have been previously assigned to methoxyl groups on pectin[57] and lignin,[50,51] respectively. The assignment of the lignin methoxyl at 56 ppm is supported by through-space proximities (3D DARR) to the lignin O-substituted aromatic carbon region of 143−157 ppm (Figure S3 of the Supporting Information). The pectin methoxyl (53 ppm), in contrast to the lignin methoxyl, shows no spatial correlation to this diffuse aromatic carbon peak in the same spectrum. Thus, 3D DARR spectra indicate that cellulose shows proximity to non-carbohydrate cell wall moieties. These are probably lignin methoxyl and protein Cα, and perhaps also some pectin methoxyl groups.

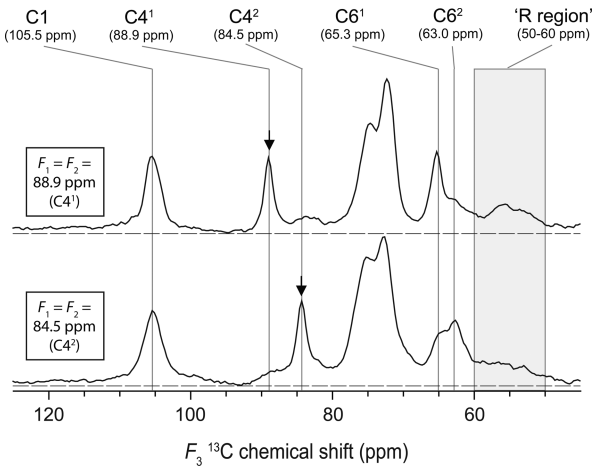

Figure 7. 1D slices from the cellulose C4 planes of the 3D 10 ms−300 ms ^{13}C−^{13}C−^{13}C DARR spectrum showing that the C4^1 cellulose at 88.9 ppm is somewhat more associated with the protein Cα and lignin methoxyl (labeled R) region than the C4^2 cellulose at 84.5 ppm.

DISCUSSION

We report here the first multidimensional ssNMR study of secondary cell wall-rich material from the model plant *Arabidopsis*. The use of ^{13}C-labeled material allowed 2D and 3D correlation spectra to be obtained. Surprisingly, a high resolution was achieved on intact dried cell walls from *Arabidopsis* stems without further sample preparation. It was possible to assign the main components of the cell walls and to detect spatial proximities, demonstrating the utility of this approach for studying the molecular architecture of plant cell walls.

Two main glucose environments in cellulose were identified [domains 1 and 2 (Figure 4)]. These have been reported to correspond to chains in the interior or on the surface of cellulose fibrils, or alternatively to crystalline and amorphous chains. They may arise from different C6 hydroxymethyl conformations[14] or from different glycosidic bond angles on interior and surface chains.[15] Using the 3D ^{13}C−^{13}C−^{13}C DARR experiment, spatial proximities were observed between glucosyl residues in the two different cellulose domains. Additionally, we identified spatial proximities between cellulose and noncarbohydrate cell wall components, probably comprising protein, lignin methoxyl, and perhaps pectin methoxyl groups [R region, 50−60 ppm (Figures 4c,d and 7)]. These are most likely protein and lignin methoxyl groups because these proximities were absent in studies of protein-extracted primary cell wall samples.[29,32]

DOI: 10.1021/bi501552k
Biochemistry 2015, 54, 2335−2345

C4[1] (C4 from cellulose domain 1, elsewhere described as "interior cellulose C4") appears to have a link to non-carbohydrate cell wall components somewhat stronger than that of C4[2] (elsewhere "surface/amorphous C4"). Dick-Perez et al.[29] found that xyloglucan in primary cell wall samples showed correlations with cellulose domain 1. Strikingly, therefore, these studies of both cell wall types suggest a closer or more abundant association of some noncellulosic components of the wall to cellulose domain 1, which appears to be inconsistent with the view that domain 1 resonances arise solely from the crystalline interior chains of cellulose. We suggest, therefore, that some glucosyl residues in surface chains may contribute to the domain 1 signal. This could occur in a number of ways. For example, different surfaces (e.g., 100 vs 010; for surface nomenclature, see ref 58), which potentially display distinct surface chemistries, hydrophilicities, and chain mobilities, might therefore allow different polysaccharide and/or C6 hydroxymethyl conformations, such that some surface chain residues have chemical shifts more similar to those of internal residues. In addition, because different residues within a single surface chain would have hydroxymethyl groups pointing in different directions [e.g., pointing toward vs pointing away from the interior of the microfibril (see 2_1 and 3_1 folds in Figure 1b)], some hydroxymethyl groups would probably exhibit a more interior-like conformation and character than others. Finally, interaction of cellulose with other polymers, for example, the hemicelluloses that are hypothesized to partially coat cellulose microfibrils, might also cause otherwise solvent-exposed surface residues to adopt "interior-like" resonances.[11,59] Similarly, secondary cell wall microfibrils can "bundle" to create larger macrofibrils, and the interacting surfaces within the macrofibril may also adopt "interior-like" resonances. Thus, we do not conclude at this point that these connections result from interactions with interior cellulose chains.

Secondary cell wall cellulose is reported to be predominantly Iβ in structure. However, we found no evidence of the characteristic Iβ C1 doublet of 104 and 107 ppm observed in 1D NMR studies of the large hydrated cellulose Iβ ribbons from the tunicate *Halocynthia*.[6,60] In our *Arabidopsis* samples, a single major C1 peak at around 105 ppm was observed, which shows through-space correlations to C4 and C6 of both putative cellulose domains. Dick-Perez et al.[29] also identified a single major C1 peak at 105 ppm from *Arabidopsis* primary cell wall samples. The absence of multiple cellulose C1 peaks in *Arabidopsis* cell wall samples may arise from factors that reduce the crystallinity of the cellulose, such as the relatively small size of *Arabidopsis* cellulose microfibrils, and the extent of cellulose interaction with other cell wall components. Drying of the sample may also cause some rearrangement of the cellulose fibrils. It will be interesting to study never-dried *Arabidopsis* stem cell wall material to investigate whether additional cellulose resonances are apparent. Indeed, Wang et al.[33] have recently observed multiple glucosyl residue environments in cellulose of never-dried grass cell wall samples.

Multiple signals from the xylosyl backbone of xylan, the main secondary cell wall hemicellulose, were identified (Figures 5 and 6). The broad nature of the peaks indicates heterogeneity in the physical environments and/or chemical structures of the xylan backbone residues. As far as heterogeneity in chemical structure is concerned, *Arabidopsis* xylan is acetylated at approximately half of the xylosyl residues and also carries [4-*O*-Me]-α-D-glucuronic acid at approximately 13% of its residues. These decorations have been observed in solution state NMR to shift the X1−X4 resonances by up to 3 ppm.[27,56] Such decorations also led to small changes in ssNMR ^{13}C shifts in grass primary cell wall samples.[33] Interestingly, however, our assignment is significantly different from these reported shifts. The discrepancy is particularly striking for X4, whose shift in solution is never greater than 77.7 ppm but in our secondary cell walls has a range of shifts extending from roughly 79 to 84 ppm, with the greatest intensity at 82.2 ppm. Because of the size of the difference in the X4 shift from solution state assignments, and the range of the shifts, xylan decorations cannot be the major cause. Changes in the helical conformation of polysaccharides are known to affect the chemical resonances of the carbons on either side of the glycosidic bonds that twist with the conformational change [C1 and C4 in a (1→4)-linked polysaccharide].[28] Indeed, it has been suggested that the 5 ppm shift in the C4 resonance between cellulose domain 1 and domain 2 may reflect alterations in glycosidic bond angles.[15] Therefore, we interpret the distinct X4 shifts observed in this work to indicate that xylan in dried *Arabidopsis* stems exists in a range of different helical conformations with very little in the 3_1 conformation found in solution xylan. The range of X1 shifts that would also be expected from a range of xylan conformations is consistent with the refocused INADEQUATE spectrum, although the evidence for a range of X1 shifts is less clear than that for X4.

One factor that might affect the helical conformation of xylan in the cell wall is interactions between xylan and cellulose that could rely on xylan adopting a 2_1 helical conformation.[26,27] Various 1D ssNMR investigations into different secondary cell wall-rich lignocellulose samples have assigned peaks in the 81.5−84 ppm region to an unknown carbon in xylan.[11,37,59,61] Moreover, very minor *J*-coupled unassigned peaks at ∼83 and ∼64 ppm, probably X4 and X5, respectively, were also seen in *Arabidopsis* primary cell wall-rich material.[29] These observations support the contention that 82−84 ppm X4 peaks may be a distinct feature of xylan in cell walls. Several of these studies explicitly assign both the ∼82 and ∼84 ppm peaks to "cellulose-aggregated xylan" on the basis of their absence in 1D NMR spectra of solution state xylan, their presence in kraft pulp, and their appearance when chemically disintegrated cotton linters (pure cellulose) were mixed with xylan.[11,59,61] However, Teleman et al.[61] also observed spectral intensity extending from the ∼75 ppm X2/X3 peak to ∼85 ppm in 1D spectra of dried extracted xylan. The signals observed in this work in dried secondary cell walls may therefore be xylan interacting with other wall components, such as cellulose, and/or dried xylan.

Our data suggest various xylan conformations can be detected in secondary plant cell walls and indicate that ssNMR is an invaluable tool for elucidating important features of plant cell wall architecture. The ability to probe unprocessed stems from the model plant *A. thaliana* with ssNMR will now allow mutant plants, for example, those deficient in cellulose and xylan, to be studied to improve our understanding of cellulose−xylan interactions.

■ ASSOCIATED CONTENT

Supporting Information

Additional results and assignment summary: monosaccharide composition of the noncrystalline polysaccharides of the *Arabidopsis* stems (Figure S1), a 2D ^{13}C−^{13}C RFDR spectrum of *Arabidopsis* secondary cell walls (Figure S2), lignin MeO at 56 ppm through-space correlations in a 2D DARR experiment (Figure S3), and solid state NMR chemical shift assignment

DOI: 10.1021/bi501552k
Biochemistry 2015, 54, 2335−2345

table (Table S1). This material is available free of charge via the Internet at http://pubs.acs.org.

AUTHOR INFORMATION

Corresponding Author

*Department of Biochemistry, University of Cambridge, Cambridge CB2 1QW, U.K. Phone: +44 1223 333340. E-mail: p.dupree@bioc.cam.ac.uk.

Author Contributions

R.D. and T.J.S. contributed equally to this work.

Funding

This work was supported by BBSRC Grant BB/G016240/1, via The BBSRC Sustainable Bioenergy Cell Wall Sugars Programme. The UK 850 MHz solid state NMR Facility was funded by EPSRC Grant EP/F017901/1 and the BBSRC, as well as the University of Warwick, including via partial funding through Birmingham Science City Advanced Materials Projects 1 and 2, by Advantage West Midlands (AWM) and the European Regional Development Fund (ERDF).

Notes

The authors declare no competing financial interest.

ACKNOWLEDGMENTS

We thank Katherine Stott (University of Cambridge) for helpful discussions and Dr. Andy Howes (University of Warwick) for expertly packing the plant stems in the NMR rotor.

ABBREVIATIONS

ssNMR, solid state nuclear magnetic resonance; CP, cross-polarization; DP, direct polarization; MAS, magic angle spinning; RFDR, radiofrequency-driven recoupling; DARR, dipolar-assisted rotational recoupling; INADEQUATE, incredible natural abundance double-quantum transfer experiment.

REFERENCES

(1) U.S. Department of Energy (2011) U.S. Billion-Ton Update: Biomass Supply for a Bioenergy and Bioproducts Industry. Technical Report ORNL/TM-2011/224 (Perlack, R. D., and Stokes, B. J., Leads) pp 227, Oak Ridge National Laboratory, Oak Ridge, TN.

(2) Carroll, A., and Somerville, C. (2009) Cellulosic Biofuels. *Annu. Rev. Plant Biol. 60*, 165−182.

(3) Carpita, N., and McCann, M. (2000) The cell wall. In *Biochemistry and Molecular Biology of Plants* (Buchanan, B. B., Wilhelm, G., and Jones, R. L., Eds.) pp 52−108, American Society of Plant Physiologists, Rockville, IL.

(4) Scheller, H. V., and Ulvskov, P. (2010) Hemicelluloses. *Annu. Rev. Plant Biol. 61* (61), 263−289.

(5) Pauly, M., and Keegstra, K. (2008) Cell-wall carbohydrates and their modification as a resource for biofuels. *Plant J. 54*, 559−568.

(6) Atalla, R. H., and Vanderhart, D. L. (1984) Native Cellulose: A Composite of 2 Distinct Crystalline Forms. *Science 223*, 283−285.

(7) Nishiyama, Y., Langan, P., and Chanzy, H. (2002) Crystal structure and hydrogen-bonding system in cellulose 1β from synchrotron X-ray and neutron fiber diffraction. *J. Am. Chem. Soc. 124*, 9074−9082.

(8) Nishiyama, Y., Sugiyama, J., Chanzy, H., and Langan, P. (2003) Crystal structure and hydrogen bonding system in cellulose 1α, from synchrotron X-ray and neutron fiber diffraction. *J. Am. Chem. Soc. 125*, 14300−14306.

(9) Sturcova, A., His, I., Apperley, D. C., Sugiyama, J., and Jarvis, M. C. (2004) Structural details of crystalline cellulose from higher plants. *Biomacromolecules 5*, 1333−1339.

(10) Driemeier, C., and Francisco, L. H. (2014) X-ray diffraction from faulted cellulose I constructed with mixed Iα-Iβ stacking. *Cellulose 21*, 3161−3169.

(11) Wickholm, K., Larsson, P. T., and Iversen, T. (1998) Assignment of non-crystalline forms in cellulose I by CP/MAS C-13 NMR spectroscopy. *Carbohydr. Res. 312*, 123−129.

(12) Atalla, R. H., and VanderHart, D. L. (1999) The role of solid state C-13 NMR spectroscopy in studies of the nature of native celluloses. *Solid State Nucl. Magn. Reson. 15*, 1−19.

(13) Foston, M. (2014) Advances in solid-state NMR of cellulose. *Curr. Opin. Biotechnol. 27*, 176−184.

(14) Newman, R. H., and Davidson, T. C. (2004) Molecular conformations at the cellulose-water interface. *Cellulose 11*, 23−32.

(15) Vietor, R. J., Newman, R. H., Ha, M. A., Apperley, D. C., and Jarvis, M. C. (2002) Conformational features of crystal-surface cellulose from higher plants. *Plant J. 30*, 721−731.

(16) Masuda, K., Adachi, M., Hirai, A., Yamamoto, H., Kaji, H., and Horii, F. (2003) Solid-state C-13 and H-1 spin diffusion NMR analyses of the microfibril structure for bacterial cellulose. *Solid State Nucl. Magn. Reson. 23*, 198−212.

(17) Newman, R. H. (2004) Homogeneity in cellulose crystallinity between samples of *Pinus radiata* wood. *Holzforschung 58*, 91−96.

(18) Vanholme, R., Demedts, B., Morreel, K., Ralph, J., and Boerjan, W. (2010) Lignin Biosynthesis and Structure. *Plant Physiol. 153*, 895−905.

(19) Van Acker, R., Vanholme, R., Storme, V., Mortimer, J. C., Dupree, P., and Boerjan, W. (2013) Lignin biosynthesis perturbations affect secondary cell wall composition and saccharification yield in *Arabidopsis thaliana*. *Biotechnol. Biofuels 6*, 46.

(20) Nishiyama, Y. (2009) Structure and properties of the cellulose microfibril. *J. Wood Sci. 55*, 241−249.

(21) Fernandes, A. N., Thomas, L. H., Altaner, C. M., Callow, P., Forsyth, V. T., Apperley, D. C., Kennedy, C. J., and Jarvis, M. C. (2011) Nanostructure of cellulose microfibrils in spruce wood. *Proc. Natl. Acad. Sci. U.S.A. 108*, E1195−E1203.

(22) Ding, S. Y., Liu, Y. S., Zeng, Y. N., Himmel, M. E., Baker, J. O., and Bayer, E. A. (2012) How Does Plant Cell Wall Nanoscale Architecture Correlate with Enzymatic Digestibility? *Science 338*, 1055−1060.

(23) Cosgrove, D. J., and Jarvis, M. C. (2012) Comparative structure and biomechanics of plant primary and secondary cell walls. *Front. Plant Sci. (Lausanne, Switz.) 3*, 204.

(24) Pu, Y. Q., Hu, F., Huang, F., Davison, B. H., and Ragauskas, A. J. (2013) Assessing the molecular structure basis for biomass recalcitrance during dilute acid and hydrothermal pretreatments. *Biotechnol. Biofuels 6*, 15.

(25) Nieduszy, I., and Marchess, Rh. (1971) Structure of β-D-(1-]4′)Xylan Hydrate. *Nature 232*, 46.

(26) Bromley, J. R., Busse-Wicher, M., Tryfona, T., Mortimer, J. C., Zhang, Z. N., Brown, D. M., and Dupree, P. (2013) GUX1 and GUX2 glucuronyltransferases decorate distinct domains of glucuronoxylan with different substitution patterns. *Plant J. 74*, 423−434.

(27) Busse-Wicher, M., Gomes, T. C. F., Tryfona, T., Nikolovski, N., Stott, K., Grantham, N. J., Bolam, D. N., Skaf, M. S., and Dupree, P. (2014) The pattern of xylan acetylation suggests xylan may interact with cellulose microfibrils as a twofold helical screw in the secondary plant cell wall of *Arabidopsis thaliana*. *Plant J. 79*, 492−506.

(28) Jarvis, M. C., and Apperley, D. C. (1995) Chain Conformation in Concentrated Pectic Gels: Evidence from C-13 Nmr. *Carbohydr. Res. 275*, 131−145.

(29) Dick-Perez, M., Zhang, Y. A., Hayes, J., Salazar, A., Zabotina, O. A., and Hong, M. (2011) Structure and Interactions of Plant Cell-Wall Polysaccharides by Two- and Three-Dimensional Magic-Angle-Spinning Solid-State NMR. *Biochemistry 50*, 989−1000.

(30) Dick-Perez, M., Wang, T., Salazar, A., Zabotina, O. A., and Hong, M. (2012) Multidimensional solid-state NMR studies of the structure and dynamics of pectic polysaccharides in uniformly C-13-labeled *Arabidopsis* primary cell walls. *Magn. Reson. Chem. 50*, 539−550.

DOI: 10.1021/bi501552k
Biochemistry 2015, 54, 2335−2345

(31) Wang, T., Zabotina, O., and Hong, M. (2012) Pectin-Cellulose Interactions in the *Arabidopsis* Primary Cell Wall from Two-Dimensional Magic-Angle-Spinning Solid-State Nuclear Magnetic Resonance. *Biochemistry 51*, 9846−9856.
(32) Wang, T., Park, Y. B., Caporini, M. A., Rosay, M., Zhong, L. H., Cosgrove, D. J., and Hong, M. (2013) Sensitivity-enhanced solid-state NMR detection of expansin's target in plant cell walls. *Proc. Natl. Acad. Sci. U.S.A. 110*, 16444−16449.
(33) Wang, T., Salazar, A., Zabotina, O. A., and Hong, M. (2014) Structure and Dynamics of *Brachypodium* Primary Cell Wall Polysaccharides from Two-Dimensional C-13 Solid-State Nuclear Magnetic Resonance Spectroscopy. *Biochemistry 53*, 2840−2854.
(34) Bootten, T. J., Harris, P. J., Melton, L. D., and Newman, R. H. (2004) Solid-state ^{13}C-NMR spectroscopy shows that the xyloglucans in the primary cell walls of mung bean (*Vigna radiata* L.) occur in different domains: A new model for xyloglucan-cellulose interactions in the cell wall. *J. Exp. Bot. 55*, 571−583.
(35) Ha, M. A., MacKinnon, I. M., Sturcova, A., Apperley, D. C., McCann, M. C., Turner, S. R., and Jarvis, M. C. (2002) Structure of cellulose-deficient secondary cell walls from the irx3 mutant of *Arabidopsis thaliana*. *Phytochemistry 61*, 7−14.
(36) Foston, M., Katahira, R., Gjersing, E., Davis, M. F., and Ragauskas, A. J. (2012) Solid-State Selective C-13 Excitation and Spin Diffusion NMR To Resolve Spatial Dimensions in Plant Cell Walls. *J. Agric. Food Chem. 60*, 1419−1427.
(37) Bardet, M., Emsley, L., and Vincendon, M. (1997) Two-dimensional spin-exchange solid-state NMR studies of C-13-enriched wood. *Solid State Nucl. Magn. Reson. 8*, 25−32.
(38) Lesage, A., Bardet, M., and Emsley, L. (1999) Through-bond carbon-carbon connectivities in disordered solids by NMR. *J. Am. Chem. Soc. 121*, 10987−10993.
(39) Komatsu, T., and Kikuchi, J. (2013) Selective Signal Detection in Solid-State NMR Using Rotor-Synchronized Dipolar Dephasing for the Analysis of Hemicellulose in Lignocellulosic Biomass. *J. Phys. Chem. Lett. 4*, 2279−2283.
(40) Tryfona, T., Liang, H. C., Kotake, T., Tsumuraya, Y., Stephens, E., and Dupree, P. (2012) Structural Characterization of *Arabidopsis* Leaf Arabinogalactan Polysaccharides. *Plant Physiol. 160*, 653−666.
(41) Bennett, A. E., Rienstra, C. M., Auger, M., Lakshmi, K. V., and Griffin, R. G. (1995) Heteronuclear Decoupling in Rotating Solids. *J. Chem. Phys. 103*, 6951−6958.
(42) Metz, G., Wu, X. L., and Smith, S. O. (1994) Ramped-Amplitude Cross-Polarization in Magic-Angle-Spinning NMR. *J. Magn. Reson., Ser. A 110*, 219−227.
(43) Fayon, F., Massiot, D., Levitt, M. H., Titman, J. J., Gregory, D. H., Duma, L., Emsley, L., and Brown, S. P. (2005) Through-space contributions to two-dimensional double-quantum J correlation NMR spectra of magic-angle-spinning solids. *J. Chem. Phys. 122*, 194313.
(44) Fung, B. M., Khitrin, A. K., and Ermolaev, K. (2000) An improved broadband decoupling sequence for liquid crystals and solids. *J. Magn. Reson. 142*, 97−101.
(45) Bennett, A. E., Ok, J. H., Griffin, R. G., and Vega, S. (1992) Chemical-Shift Correlation Spectroscopy in Rotating Solids: Radio Frequency-Driven Dipolar Recoupling and Longitudinal Exchange. *J. Chem. Phys. 96*, 8624−8627.
(46) Takegoshi, K., Nakamura, S., and Terao, T. (2001) C-13-H-1 dipolar-assisted rotational resonance in magic-angle spinning NMR. *Chem. Phys. Lett. 344*, 631−637.
(47) Li, S. H., Zhang, Y., and Hong, M. (2010) 3D C-13-C-13-C-13 correlation NMR for de novo distance determination of solid proteins and application to a human α-defensin. *J. Magn. Reson. 202*, 203−210.
(48) Brown, D. M., Goubet, F., Vicky, W. W. A., Goodacre, R., Stephens, E., Dupree, P., and Turner, S. R. (2007) Comparison of five xylan synthesis mutants reveals new insight into the mechanisms of xylan synthesis. *Plant J. 52*, 1154−1168.
(49) Harholt, J., Suttangkakul, A., and Scheller, H. V. (2010) Biosynthesis of Pectin. *Plant Physiol. 153*, 384−395.
(50) Hatcher, P. G. (1987) Chemical Structural Studies of Natural Lignin by Dipolar Dephasing Solid-State C-13 Nuclear-Magnetic-Resonance. *Org. Geochem. 11*, 31−39.
(51) Holtman, K. M., Chen, N., Chappell, M. A., Kadla, J. F., Xu, L., and Mao, J. D. (2010) Chemical Structure and Heterogeneity Differences of Two Lignins from Loblolly Pine As Investigated by Advanced Solid-State NMR Spectroscopy. *J. Agric. Food Chem. 58*, 9882−9892.
(52) Hongo, S., Sato, K., Yokoyama, R., and Nishitani, K. (2012) Demethylesterification of the Primary Wall by PECTIN METHYLESTERASE35 Provides Mechanical Support to the Arabidopsis Stem. *Plant Cell 24*, 2624−2634.
(53) Cadars, S., Mifsud, N., Lesage, A., Epping, J. D., Hedin, N., Chmelka, B. F., and Emsley, L. (2008) Dynamics and disorder in surfactant-templated silicate layers studied by solid-state NMR dephasing times and correlated line shapes. *J. Phys. Chem. C 112*, 9145−9154.
(54) Cadars, S., Lesage, A., and Emsley, L. (2005) Chemical shift correlations in disordered solids. *J. Am. Chem. Soc. 127*, 4466−4476.
(55) Sakellariou, D., Brown, S. P., Lesage, A., Hediger, S., Bardet, M., Meriles, C. A., Pines, A., and Emsley, L. (2003) High-resolution NMR correlation spectra of disordered solids. *J. Am. Chem. Soc. 125*, 4376−4380.
(56) Chong, S. L., Virkki, L., Maaheimo, H., Juvonen, M., Derba-Maceluch, M., Koutaniemi, S., Roach, M., Sundberg, B., Tuomainen, P., Mellerowicz, E. J., and Tenkanen, M. (2014) O-Acetylation of glucuronoxylan in *Arabidopsis thaliana* wild type and its change in xylan biosynthesis mutants. *Glycobiology 24*, 494−506.
(57) Ng, J. K. T., Zujovic, Z. D., Smith, B. G., Johnston, J. W., Schroder, R., and Melton, L. D. (2014) Solid-state C-13 NMR study of the mobility of polysaccharides in the cell walls of two apple cultivars of different firmness. *Carbohydr. Res. 386*, 1−6.
(58) Matthews, J. F., Skopec, C. E., Mason, P. E., Zuccato, P., Torget, R. W., Sugiyama, J., Himmel, M. E., and Brady, J. W. (2006) Computer simulation studies of microcrystalline cellulose Iβ. *Carbohydr. Res. 341*, 138−152.
(59) Larsson, P. T., Hult, E. L., Wickholm, K., Pettersson, E., and Iversen, T. (1999) CP/MAS C-13-NMR spectroscopy applied to structure and interaction studies on cellulose I. *Solid State Nucl. Magn. Reson. 15*, 31−40.
(60) Malm, E., Bulone, V., Wickholm, K., Larsson, P. T., and Iversen, T. (2010) The surface structure of well-ordered native cellulose fibrils in contact with water. *Carbohydr. Res. 345*, 97−100.
(61) Teleman, A., Larsson, P. T., and Iversen, T. (2001) On the accessibility and structure of xylan in birch kraft pulp. *Cellulose 8*, 209−215.

DOI: 10.1021/bi501552k
Biochemistry 2015, 54, 2335−2345